

## Laser-induced fluorescence measurements of buoyancy driven mixing in tilted tubes

T. Séon,<sup>a)</sup> J.-P. Hulin, and D. Salin

*Laboratoire Fluides Automatique et Systèmes Thermiques, UMR 7608, CNRS, Universités P. et M. Curie and Paris Sud, Bâtiment 502, Campus Universitaire, 91405 Orsay Cedex, France*

B. Perrin

*Laboratoire Pierre Aigrain, UMR 8551, CNRS, Ecole Normale Supérieure, Département de Physique, 24 rue Lhomond, 75231 Paris Cedex 05, France*

E. J. Hinch

*DAMTP-CMS, University of Cambridge, Wilberforce Road, Cambridge CB3 0WA, United Kingdom*

(Received 29 December 2005; accepted 27 February 2006; published online 12 April 2006)

The front of a light fluid rising into a miscible heavier fluid inside a long tilted tube has been analyzed by laser-induced fluorescence. Both the local concentration field and the front velocity  $V_f$  have been studied in the inertial flow regime as a function of the tilt angle  $\theta$  for a constant density contrast ( $At=4 \times 10^{-3}$ ). We demonstrate experimentally that the velocity  $V_f$  is directly related to the local density contrast  $C_f$  by the relation  $V_f \propto (C_f)^{0.5}$ . This relation reflects a local instantaneous equilibrium between inertia and buoyancy; it is valid in the transient relaxation phase as well as in the quasistationary regime reached thereafter. © 2006 American Institute of Physics.

[DOI: [10.1063/1.2189286](https://doi.org/10.1063/1.2189286)]

The present Letter analyzes the motion of a light fluid rising inside a heavier, miscible one inside a long tilted tube as frequently occurs in chemical and petroleum engineering; closely related problems include gravity currents and lock exchange processes.<sup>1-3</sup> More specifically, it will be shown by means of direct concentration measurements that the velocity  $V_f$  of the front of each fluid penetrating into the other is directly related to the local density contrast between fluids on both sides of the front.

For immiscible fluids, many papers<sup>4-6</sup> studied the related problem of large gas bubbles rising in long tubes. For large tube diameters  $d$  and long bubbles, their velocity  $V_b$  follows the scaling law  $V_b \propto (gd)^{0.5}$  both for vertical and tilted tubes. This reflects a balance between inertial and buoyancy terms respectively proportional to  $\rho V_f^2$  and  $\rho gd$  leading to a characteristic velocity,

$$V_t = \sqrt{Atgd}. \quad (1)$$

The Atwood number  $At$  is the ratio of the difference  $\Delta\rho$  of the densities of the two fluids by their sum with  $At \approx 1$  for a gas bubble (in gravity current studies,  $g' = 2gAt$  is used instead of  $At$ ).

For miscible fluids, the penetration front dynamics will be influenced by mixing between the two fluids both at the front and behind it: most of this mixing will result from the Kelvin-Helmholtz instabilities induced by the relative shear motion of the two fluids. Their appearance depends also on the segregation induced by the transverse gravity component in tilted tubes<sup>7,8</sup> and, therefore, on the tilt angle  $\theta$  from vertical.

In a previous work,<sup>9</sup> the variation with  $\theta$  of the stationary front velocity  $V_{f\infty}$  at long times was observed to display three different regimes. Close to vertical,  $V_{f\infty}$  increases with the tilt angle  $\theta$ : in this regime 1, strong transverse mixing takes place due to Kelvin-Helmholtz instabilities. As  $\theta$  increases, segregation effects become stronger and mixing is less efficient:  $V_{f\infty}$  reaches a plateau value equal to  $0.7 \times V_t$  (regime 2). Finally, as  $\theta$  increases further towards the horizontal (regime 3), there is a parallel, Poiseuille-like, counterflow of the two fluids with no mixing and  $V_f$  decreases: the buoyancy potential energy is then dissipated by viscosity. In regime 2, the proportionality of the front velocity  $V_{f\infty}$  to  $V_t$  suggests, on the contrary, that  $V_{f\infty}$  is determined, as for a gas bubble, by a balance between buoyancy and inertia. It also suggests that the local density contrast  $\delta\rho$  at the front is equal to the density difference  $\Delta\rho$  between the fluids. In regime 1, the lower value of  $V_{f\infty}$  indicates that, due to mixing, the local density contrast  $\delta\rho$  at the front is smaller than  $\Delta\rho$ . This is confirmed by the increase of  $V_{f\infty}$  with  $\mu$  in regime 1 at constant values of  $At$  and  $\theta$ : mixing becomes less efficient and  $\delta\rho$  becomes closer to  $\Delta\rho$ .

The objective of this Letter is to check quantitatively these assumptions. The variation of the local relative fraction at the front is directly measured by laser-induced fluorescence (LIF): this allows us to estimate the corresponding local density contrast  $\delta\rho$  and to compare its variations with  $\theta$  to those of the front velocity  $V_f$  (the study is performed in regimes 1 and 2 where the front dynamics is controlled by inertia). Another important feature is the transient phase of the front motion before it reaches a stationary velocity.

The study is performed in a 4-m-long transparent tube with an internal diameter  $d=20$  mm that can be tilted to all angles between vertical and horizontal. Initially, the heavier

<sup>a)</sup>Electronic mail: seon@fast.u-psud.fr

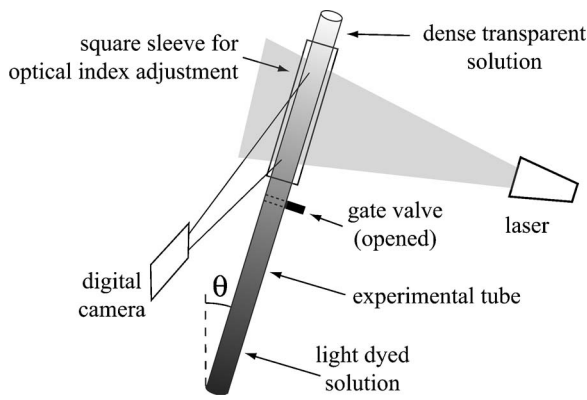


FIG. 1. Schematic view of experimental setup.

and lighter fluids are, respectively, located in the upper and lower halves of the tube and separated by a gate valve (Fig. 1). The tube is illuminated sideways by a 1-mm-thick vertical green laser sheet ( $\lambda=532$  nm) that contains the tube axis. After opening the gate valve, pictures are taken at regular intervals (0.5 or 0.75 s) using a digital camera with a high stability and dynamic range<sup>10,11</sup> facing the tube and the light plane. The lighter fluid is water dyed with 50 mg/l of fluorescein while the heavier one is a  $\text{CaCl}_2$ -water solution: only regions of the laser sheet containing some dyed fluid appear as illuminated in the pictures. Light absorption measurements used previously<sup>10,12</sup> gave an average value of the concentration along the path of the light through the tube; in contrast, the present measurements provide a local concentration map in the diametral plane of the tube illuminated by the laser. The field of view is 600 mm long and its lower boundary is located at 200 mm above the gate valve (this region of interest is initially saturated only with the heavy transparent solution). In order to reduce the cylindrical lens effect due to the tube geometry, the part corresponding to the field of view is enclosed inside a larger tube with a square cross section: the space between both tubes is filled with water and two of the sides of the square tube are parallel to the light plane. The relative reflective index contrast between the salt solutions and the water outside the tube is of the order of  $1.5 \times 10^{-3}$  and can be neglected.<sup>13</sup> The optical index difference ( $\delta n=0.14$ ) between the liquids and the tube wall induces a small increase of the apparent radius of the tube (by typ. 1 mm) but does not influence the local concentration measurements in the region of interest. All fluids are degassed and filtered to eliminate bubbles and solid particles in order to eliminate unwanted light diffusion.

In order to obtain quantitative values of the local relative fraction of the fluids, images provided by the digital camera are normalized between reference images obtained for the experimental tube filled, respectively, with the heavy (transparent) and light (fluorescent) fluids. The linear dependence of the intensity in the normalized images on the concentration of fluorescein is checked through calibrations with solutions of different concentrations realized *in situ* directly on the experimental setup (the variation is linear with a slope constant to within 2%). In the following, one therefore assumes that these normalized images provide directly the lo-

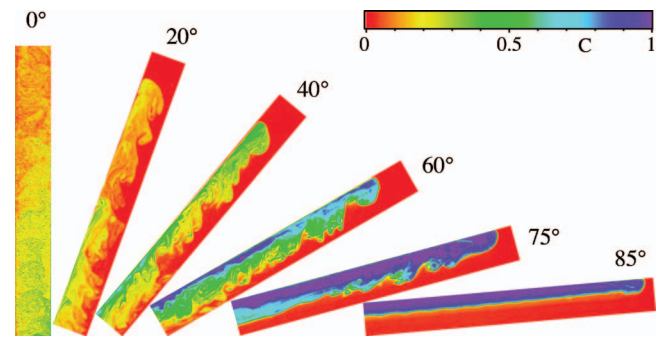


FIG. 2. (Color) Images of the normalized relative fraction of light fluid obtained at different tilt angles  $\theta=0^\circ$ ,  $20^\circ$ ,  $40^\circ$ ,  $60^\circ$ ,  $75^\circ$ , and  $85^\circ$  (field of view= $20 \times 300$  mm). The color code for the normalized fraction is shown at the top right of the figure. The magnification of the images of the tube is higher perpendicular compared to parallel to the tube axis.

cal relative fraction  $C(\mathbf{x}, t)$  of light fluid in the beam plane (the components of  $\mathbf{x}$  are the coordinates of a point in the beam plane). This amounts to neglecting the molecular diffusion of salt and dye between the two solutions. The fluorescein concentration is chosen both to be high enough to have a detectable fluorescence and low enough to avoid light absorption. Assuming that the local density of the mixture varies linearly with  $C(\mathbf{x}, t)$ , the variations of  $C$  can be translated into density variations: in particular, the value  $C_f$  of the relative fraction  $C(\mathbf{x}, t)$  at the front is equal to the ratio  $\delta\rho/\Delta\rho$  of the local density contrast and the density difference between both fluids.

Figure 2 displays images of the normalized fraction of light fluid in the experimental zone at different tilt angles for the same density contrast  $At=4 \times 10^{-3}$  and a viscosity  $\mu=10^{-3}$  Pa.s equal for all fluids: with the color code used, the heavier transparent fluid appears in red and the lighter fluorescent one in dark blue. Mixtures of the two fluids appear in intermediate colors. Note that the observation zone is above the gate valve; symmetrical observations might be performed below on the penetration front of the heavier fluid.

Figure 2 demonstrates the segregation induced by tilting the tube. For large  $\theta$  values ( $\theta=85^\circ$  in Fig. 2), the transverse gravity component is large enough to prevent the development of Kelvin-Helmholtz instabilities and keep the light and heavy fluids separated. For  $\theta=75^\circ$ , an instability takes place and a mixing zone develops downstream of the front. There is, however, on the upper side of the tube, a channel inflow of pure light fluid allowing it to maintain its relative fraction at the front equal to 1. As  $\theta$  decreases below  $60^\circ$ , mixing becomes more efficient and the relative light fluid concentration at the front becomes less than 1. For lower tilt angles, such as  $\theta=20^\circ$ , there remains, however, a transverse concentration gradient across the tube section: the higher concentration of light fluid on the upper side of the tube results in a local upwards flow of this fluid. This maintains a relatively high density contrast at the front.

In order to analyze quantitatively these results, the typical relative fraction at the front  $C_f(t)$  inside the lighter fluid has been determined by averaging six profiles of the concentration along the tube located in the region of highest concentration of the tube section (these profiles cover about one

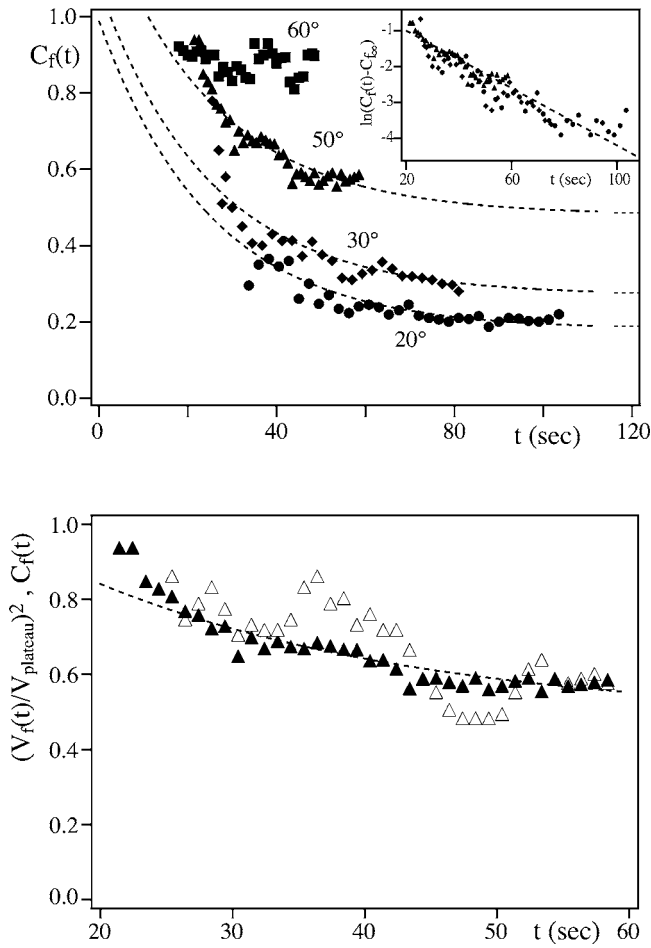


FIG. 3. (a) Time variations of the characteristic relative fraction  $C_f(t)$  at the front for four different tilt angles  $\theta=20^\circ$  ( $\bullet$ ),  $30^\circ$  ( $\blacklozenge$ ),  $50^\circ$  ( $\blacktriangle$ ), and  $60^\circ$  ( $\blacksquare$ ). Dashed lines: exponential relaxations of time constant  $\tau=25$  s (see inset) towards asymptotic values 0.18, 0.27, and 0.48 (straight horizontal segments). (b) Compared time variations of the relative fraction  $C_f(t)$  ( $\blacktriangle$ ) and of the square of the normalized instantaneous front velocity  $[V_f(t)/V_{\text{plateau}}]^2$  ( $\triangle$ ) for  $\theta=50^\circ$ .

tenth of the diameter): the maximum of this concentration profile located closest to the front will be considered as representing the concentration  $C_f(t)$  at the front. Beyond the front, in the heavy fluid, the images of Fig. 2 indicate that there is no mixing with the lighter fluid: the concentration of the lighter fluid is then assumed to be zero and the relative density contrast between the two sides of the front is taken equal to  $C_f$ . Also, the front is assumed to be located at the point of the averaged profiles where the concentration becomes zero. This procedure has been applied to successive images in order to determine the time variations of both the instantaneous relative fraction  $C_f$  at the front and its instantaneous velocity  $V_f$  (deduced from the displacement between two images).

Figure 3(a) displays the variation of  $C_f(t)$  with time for different angles  $\theta$  ranging from  $20^\circ$  to  $60^\circ$  (note that the range of the plot corresponds to times during which the front is located inside the field of view of the camera). One observes that, after an initial decrease,  $C_f(t)$  reaches a roughly constant value  $C_{f\infty}$ . One reaches therefore a flow regime which appears as stationary over the time scale of the experi-

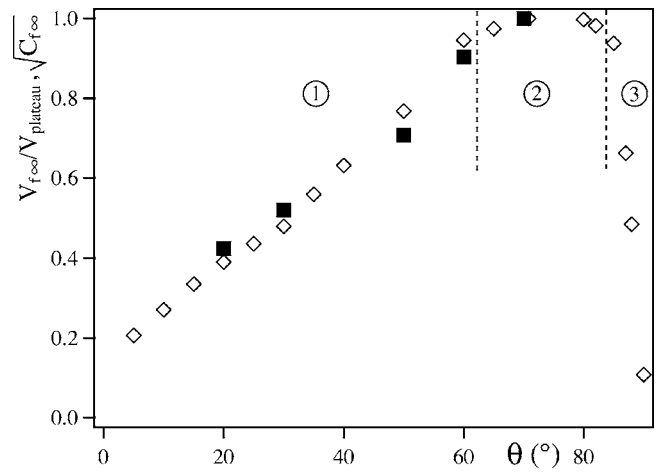


FIG. 4. Compared variations with the tilt angle  $\theta$  of the experimental normalized stationary front velocity  $V_{f\infty}/V_{\text{plateau}}$  ( $\diamond$ ) and of  $\sqrt{C_{f\infty}}$  ( $\blacksquare$ ) computed from concentrations measured experimentally (the values of  $\mu$  and  $At$  are the same as in Figs. 2 and 3).

ment: this is made possible by the inflow of light fluid near the upper side of the tube.

As can be seen by extrapolating the variations of  $C_f$  with time for  $\theta=30^\circ$  and  $50^\circ$  in Fig. 3(a),  $C_f(t)$  starts to decrease below 1 only after a finite time increasing with  $\theta$ . Then,  $C_f(t)$  relaxes towards the limiting value  $C_{f\infty}$ : the linear variation of  $\ln[C_f(t) - C_{f\infty}]$  in the inset of Fig. 3(a) suggests an exponential relaxation with a characteristic time  $\tau=25\pm 5$  s independent of  $\theta$  within experimental error. Note that  $\tau$  is much longer than, for instance, the typical duration  $[d/(Atg)]^{0.5} \approx 0.7$  s of convective motions. A closer study of the characteristic times of energy dissipation and mixing processes in these flows is therefore needed.

The limiting value  $C_{f\infty}$  increases with  $\theta$ , reflecting the decreasing efficiency of mixing at the front. This variation allows one to check quantitatively that the front velocity  $V_f$  is determined as expected by the corresponding local density contrast  $\delta\rho$ . One should indeed have  $\delta\rho=C_f \times \Delta\rho$  so that, from Eq. (1), the relation  $V_f \propto V_t$  would become in the stationary regime,

$$V_{f\infty} \propto \sqrt{AtC_{f\infty}gd}. \tag{2}$$

Since the plateau velocity  $V_{\text{plateau}}$  must correspond to  $C_{f\infty} = 1$  ( $\delta\rho = \Delta\rho$ ), one has [assuming that the proportionality constant is independent of  $\theta$  in Eq. (2)],

$$\frac{V_{f\infty}}{V_{\text{plateau}}} = \sqrt{C_{f\infty}}. \tag{3}$$

Figure 4 tests the validity of this relation by displaying the variations of  $\sqrt{C_{f\infty}}$  with  $\theta$  measured in the present work together with the variation with  $\theta$  of the ratio  $V_{f\infty}/V_{\text{plateau}}$  reported in Ref. 9 (these values are more precise than those determined in the present work due to their determination over a larger path length). There is indeed a close agreement between the variations of  $\sqrt{C_{f\infty}}$  with the tilt angle  $\theta$  and those of  $V_{f\infty}/V_{\text{plateau}}$ ; furthermore, in the plateau region,  $C_{f\infty}$  is very close to 1. This confirms our assumptions on the variation of the stationary front velocity with the local density contrast.

A similar comparison can be made for the instantaneous values of the density contrast and the front velocity during the transient phase. The variations of the normalized velocity squared  $[V_f(t)/V_{\text{plateau}}]^2$  with time for  $\theta=50^\circ$  are plotted in Fig. 3(b) together with those of the concentration  $C_f(t)$ . The global variation of both variables is the same. The deviations from this common decreasing trend are larger for the velocity than for the concentration: they are due to bursts of lighter fluid arriving at the front (similar front velocity variations have been observed in experiments on lock-exchange flows in a sloping channel<sup>14</sup>). Equation (3) is therefore also valid for the instantaneous values of the front velocity and of the density contrast: this indicates that an equilibrium between buoyancy and inertia forces resulting in a quasistationary front motion is obtained after a time much shorter than that ( $\tau=25$  s) needed to reach the limiting asymptotic front velocity [Figs. 3(a) and 3(b)].

To conclude, direct local concentration measurements have been achieved with the LIF technique on a front of light fluid rising into a heavier miscible one in long tilted tubes: these experiments have allowed us to characterize quantitatively the close relationship between the degree of mixing close to the front and the front velocity in flow regimes for which inertia is predominant. These measurements have demonstrated that, after a transient phase during which both front velocity  $V_f$  and the local concentration  $C_f$  of invading fluid decrease with time, a quasistationary regime in which both  $V_f$  and  $C_f$  are constant is reached (note that  $C_f$  starts to decrease from 1 only after a delay). A key result from these experiments is the proportionality of the front velocity  $V_f$  to the square root of the concentration  $C_f$  for given  $At$  and  $\theta$  values both in the stationary and in the transient regimes.

These results raise important questions regarding the scaling laws relating the concentration at the front, the tilt angle, and other parameters such as the density contrast between the fluids and their viscosity. It will be important to characterize with a high resolution spatial and temporal variations of mixing in these flows, using, for example, tools already applied to the early stages of Rayleigh-Taylor flows.<sup>15</sup> Understanding the instabilities generating this mixing is also needed; in particular, through an analysis of the flow velocity field similar to that presented here for the con-

centration. Another important issue is the dynamics of the front at long times. The fact that  $V_f$  (and therefore  $C_f$ ) are constant with time after an initial transient phase implies that the global amount of transverse mixing remains the same although the length of the mixing zone increases. The efficiency of transverse mixing per unit length must therefore decrease: this should be checked at longer times (and therefore for longer tubes) over which the front velocity may no longer be constant. Finally, the characteristic duration of the transient phase has been found to be  $\approx 25$  s, independent of the tilt angle: experiments with different tube radii and fluid viscosities will be necessary to understand the meaning of this value.

We thank G. Chauvin and R. Pidoux for designing and realizing the experimental setup.

<sup>1</sup>T. B. Benjamin, "Gravity currents and related phenomena," *J. Fluid Mech.* **31**, 209 (1968).

<sup>2</sup>J. O. Shin, S. B. Dalziel, and P. F. Linden, "Gravity currents produced by lock exchange," *J. Fluid Mech.* **521**, 1 (2004).

<sup>3</sup>C. Härtel, E. Meiburg, and F. Necker, "Analysis and numerical simulation of the flow at a gravity-current head. Part 1. Flow topology and front speed for slip and no-slip boundaries," *J. Fluid Mech.* **418**, 189 (2000).

<sup>4</sup>R. M. Davies and G. I. Taylor, "The mechanics of large bubbles rising through extended fluids and through liquids in a tube," *Proc. R. Soc. London, Ser. A* **200**, 375 (1950).

<sup>5</sup>E. E. Zukoski, "The influence of viscosity, surface tension and inclination angles on the motion of long bubbles in closed tubes," *J. Fluid Mech.* **25**, 821 (1966).

<sup>6</sup>C. Clanet, P. Héraud, and G. Searby, "Rising velocities of bubbles," *J. Fluid Mech.* **519**, 359 (2004).

<sup>7</sup>G. A. Lawrence, F. K. Browand, and L. G. Redekopp, "The stability of the sheared density interface," *Phys. Fluids A* **3**, 2360 (1991).

<sup>8</sup>E. J. Strang and H. J. S. Fernando, "Entrainment and mixing in stratified shear flows," *J. Fluid Mech.* **428**, 349 (2001).

<sup>9</sup>T. Seon, D. Salin, J. P. Hulin, B. Perrin, and E. J. Hinch, "Buoyancy driven front dynamics in tilted tubes," *Phys. Fluids* **17**, 031702 (2005).

<sup>10</sup>M. Debacq, V. Fanguet, J. P. Hulin, D. Salin, and B. Perrin, "Self-similar concentration profiles in buoyant mixing of miscible fluids in a vertical tube," *Phys. Fluids* **13**, 3097 (2001).

<sup>11</sup>Coolsnap FX camera, Roper Scientific, Photometrics Division.

<sup>12</sup>T. Seon, J. P. Hulin, D. Salin, B. Perrin, and E. J. Hinch, "Buoyant mixing of miscible fluids in tilted tubes," *Phys. Fluids* **16**, L103 (2004).

<sup>13</sup>*CRC Handbook of Chemistry and Physics*, 63rd ed. (CRC, Boca Raton, FL, 1982), pp. C-782 and D-733.

<sup>14</sup>P. F. Linden (private communication).

<sup>15</sup>D. L. Youngs, "Three-dimensional numerical simulation of turbulent mixing by Rayleigh-Taylor instability," *Phys. Fluids A* **3**, 1312 (1991).